Quantized Field-Effect Tunneling between Topological Edge or Interface States

Yong Xu,[1,2] Yan-Ru Chen,[1,2] Jun Wang,[3] Jun-Feng Liu,[1,2,*] and Zhongshui Ma[4,5,†]

[1]*School of Physics and Electronic Engineering, Guangzhou University, Guangzhou 510006, China*
[2]*Department of Physics, Southern University of Science and Technology, Shenzhen 518055, China*
[3]*Department of Physics, Southeast University, Nanjing 210096, China*
[4]*School of Physics, Peking University, Beijing 100871, China*
[5]*Collaborative Innovation Center of Quantum Matter, Beijing 100871, China*

(Received 9 January 2019; revised manuscript received 8 September 2019; published 12 November 2019)

We study the tunneling through a two-dimensional topological insulator with topologically protected edge states. It is shown that the tunneling probability can be quantized in a broad parameter range, 0 or 1, tuned by an applied transverse electric field. Based on this field-effect tunneling, we propose two types of topological transistors based on helical edge or interface states of quantum spin Hall insulators separately. The quantized tunneling conductance is obtained and shown to be robust against nonmagnetic disorders. Usually, the topological transition is necessary in the operation of topological transistors. These findings provide a new strategy for the design of topological transistors without topological transitions.

DOI: 10.1103/PhysRevLett.123.206801

Introduction.—It is well known that the tunneling probability is usually very small and decays exponentially with the transport length in a normal insulator. One may wonder what the tunneling is like through a topological insulator (TI) in the presence of transverse surface or edge states. It is intuitively supposed that the coupling between two surface states at opposite surfaces is capable of an important role in the tunneling. It has been shown [1] that the coupling between the surface states at two opposite surfaces opens a gap in the surface states due to the so-called finite-size effect. The tunneling between Fermi-arc surface states through Weyl points is recently verified by the theoretical prediction [2] and the experimental observation of three-dimensional quantum Hall effect [3–5] in Weyl semimetals. The natural question is whether the perfect tunneling is possible between the edge or surface states at two opposite edges or surfaces in a gapped topological insulator.

In addition to providing dissipationless transport channels, TIs are also used to design topological transistors [6–12] in device applications for the benefit of robustness against impurity scattering. In such topological transistors, the off state is usually realized by opening a gap in the edge channels through a topological phase transition or the finite-size effect. The topological phase transitions have been suggested to be controlled by an electric field [7–13], a magnetic field [13–15], a strain [16], or even the pressure and temperature [17,18]. However, the experimental realization of the electric manipulation of topological transitions is still a challenge. Further, the gap opened by the finite-size effect is very small. It implies that the off state requires fine-tuning of the chemical potential and a very low temperature in longitudinal tunneling transistors along edge channels. Additionally, the nonlocal transistor based on the coupling of edge or surface states [19,20], the topological spin transistor based on spin [21–23], and the imperfect transistor based on the modulation of impurity scattering [24] have also been discussed.

In this Letter, we show that the tunneling between the edge or surface states at opposite boundaries can be perfect and tunable from 0 to 1 by an electric field. This transverse tunneling effect provides a new strategy for the design of topological transistors without topological transitions. We propose two types of transverse tunneling transistors based on helical edge and interface states of quantum spin Hall insulators separately and determine the conditions of quantized conductance for the on or off state, respectively. Compared with longitudinal tunneling transistors along edge channels, such transverse tunneling transistors overcome the challenge of fine-tuning of the chemical potential to reside in the small finite-size induced gap.

Tunneling between topological edge states.—We start by considering the tunneling between topological surface states. For simplicity, we consider a two-dimensional topological insulator (2DTI) such as HgTe/CdTe quantum wells [25–27]. When the Fermi energy lies inside the bulk gap, only the helical edge modes are responsible for the transport. In the absence of magnetic impurities, two sets of chiral edge states are degenerate for spin-up and spin-down electrons. Therefore, we consider only the tunneling between spin-down edge states. The physics is the same for spin-up edge states but with opposite chirality. In a 2DTI ribbon shown in Fig. 1(a), two chiral spin-down edge modes are coupled by the finite-size effect. The effective model used to describe the coupling can be written as

 © 2019 American Physical Society

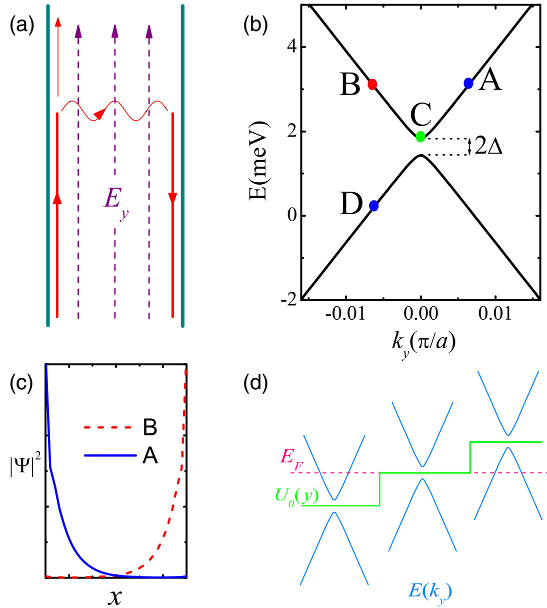

FIG. 1. (a) Sketch of the tunneling between topological edge states in a 2DTI under an electric field E_y. Only spin-down edge states are shown. (b) The band structure shows a gap due to the finite-size effect. (c) The wave function distributions of states A and B marked in (b). (d) The linear electrostatic potential U_y induced by the uniform electric field E_y can be simplified and modeled by two step functions.

$$H = \begin{pmatrix} \hbar v_F k & \Delta \\ \Delta & -\hbar v_F k \end{pmatrix}, \tag{1}$$

where $\pm\hbar v_F k$ denote the edge states at two edges and Δ describes the coupling between them. The finite-size induced gap Δ is related to the bulk gap Δ_0 by $\Delta = \Delta_0 e^{-2L/\xi}$ [28], where L is the width of the ribbon, and $\xi = \hbar v_F/\Delta_0$ is the penetration depth of the edge states. By solving the eigenproblem, we have eigenenergies $E_\pm = \pm\sqrt{\hbar^2 v_F^2 k^2 + \Delta^2}$ and corresponding eigenwave functions

$$\psi_\pm = \frac{1}{\sqrt{u^2 + \Delta^2}} \begin{pmatrix} \Delta \\ u \end{pmatrix} e^{iky} \tag{2}$$

with $u = E_\pm - \hbar v_F k$.

It is shown in Fig. 1(b) that the edge states are gapped by the finite-size effect. We consider the motion of an electron in the initial state A in the presence of an electric field E_y along the y direction. According to the equation of motion $\dot{k} = -eE_y/\hbar$, the electron will be slowed down by the electrostatic force and get to state C. Then the electron will either get to state B or cross the gap to get to state D. Figure 1(c) shows that states A and D locate at the left edge, while B locates at the right edge. If the electron evolves from state A to state B, it tunnels from the left edge to the right edge through the insulating bulk.

Beyond this semiclassical picture, we can also evaluate the probabilities of two processes by revisiting the evolution as a quantum scattering problem. The linear electrostatic potential induced by the uniform electric field can be simplified and modeled by two step functions, i.e., $U(y) = E[\Theta(y) + \Theta(y - w)]$, where E is the energy of the incident electron and $y \in [0, w]$ is the range in which the energy is inside the gap, as sketched in Fig. 1(d). We argue that this approximation is valid because the scattering will be possible only when the energy is around the gap. Far away from the gap, the coupling between the edge states at two sides will vanish and the scattering will be forbidden. For $y < 0$, the wave function is written as

$$\psi(y) = \begin{pmatrix} \Delta \\ u \end{pmatrix} e^{iky} + r \begin{pmatrix} u \\ \Delta \end{pmatrix} e^{-iky}, \tag{3}$$

where the wave vector $k = \sqrt{E^2 - \Delta^2}/(\hbar v_F)$ and $u = E - \hbar v_F k$. For simplicity, we consider only the situation of $E > 0$. In the area $y \in [0, w]$, the kinetic energy is zero and the wave function reads

$$\psi(y) = a \begin{pmatrix} 1 \\ -i \end{pmatrix} e^{-\Delta y/(\hbar v_F)} + b \begin{pmatrix} 1 \\ i \end{pmatrix} e^{\Delta y/(\hbar v_F)}. \tag{4}$$

For $y > w$, the wave function is

$$\psi(y) = t \begin{pmatrix} \Delta \\ -u \end{pmatrix} e^{-iky}. \tag{5}$$

By the continuity of the wave function at $y = 0$ and $y = w$, we can obtain the transverse transmission probability as follows:

$$T_y = |t|^2 = \frac{E^2 - \Delta^2}{E^2 \cosh^2[\Delta w/(\hbar v_F)]}. \tag{6}$$

Note that the tunneling probability along the x direction should be defined as $T_x = |r|^2 = 1 - T_y$. From Eq. (6), we can clearly see that the quantized tunneling will happen when $\Delta w/(\hbar v_F) \gg 1$. However, the tunneling probability will be very small when the electric field is absent. It formulates that the tunneling probability can be modulated by the transverse electric field.

Topological transistor based on edge state tunneling.— Based on this field-effect tunneling of edge states, we propose a topological transistor as shown in Fig. 2(a). In such an inverted T-shaped junction, a 2DTI quantum wire is connected with two metallic leads at the foot. The incident electron from the left lead first moves upward by means of the left edge state. Under the modulation of a transverse electric field, the electron may tunnel to the right side completely or do not tunnel at all. The conductance of the junction will be a conductance quantum for the former

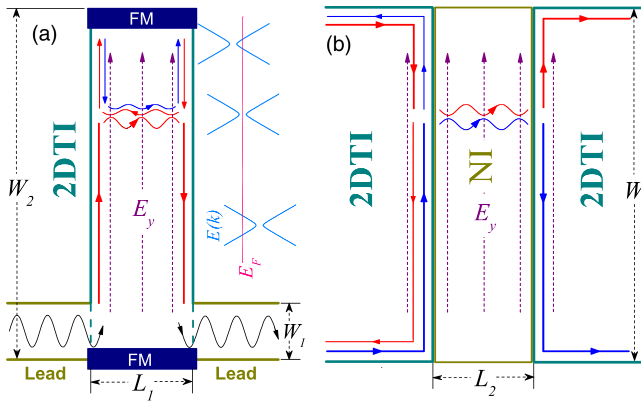

FIG. 2. Sketch of topological transistors based on (a) edge state and (b) interface state tunneling. In (a), a 2DTI quantum wire is connected with two metallic leads at the foot. Two ferromagnets (FMs) are deposited at the top and bottom of the wire to gap the edge channel. In (b), a normal insulator quantum wire are sandwiched between two 2DTI leads. The transverse electric field E_y is used to assist the tunneling between topological edge or interface states located at two edges or interfaces.

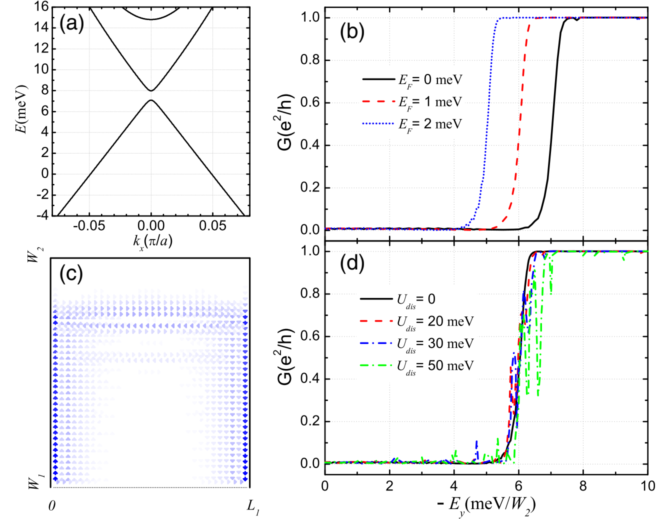

FIG. 3. Numerical results for the topological transistor based on edge state tunneling shown in Fig. 2(a). (a) Dispersion of edge states in a 2DTI quantum wire with the width $L_1 = 31a$. (b) Conductance as a function of the transverse electric field E_y for three chosen Fermi energies $E_F = 0$, 1, and 2 meV. Note that E_y is negative. (c) Current distribution for $E_F = 1$ meV and $E_y = 8$ meV. (d) Conductance in the presence of nonmagnetic disorders with various disorder strengths $U_{\rm dis}$ for $E_F = 1$ meV. Structure parameters are $W_1 = 30a$, $W_2 = 4000a$, and $L_1 = 31a$.

case, and zero for the latter case. To break the connectivity between the left and right edge states, two ferromagnets are deposited at the top and bottom of the wire to gap the edge channel.

We take HgTe/CdTe quantum wells as an example of the 2DTI. The effective Hamiltonian reads

$$H_{TI} = \epsilon(k) + \begin{pmatrix} M(k) & Ak_+ & 0 & 0 \\ Ak_- & -M(k) & 0 & 0 \\ 0 & 0 & M(k) & -Ak_- \\ 0 & 0 & -Ak_+ & -M(k) \end{pmatrix}, \quad (7)$$

where $\epsilon(k) = C - D(k_x^2 + k_y^2)$, $M(k) = M_0 - B(k_x^2 + k_y^2)$, and $k_\pm = k_x \pm ik_y$. In our calculation, the material parameters are taken as $A = 364.5$ meV nm, $B = -686$ meV nm^2, $C = 0$, $D = -512$ meV nm^2, and $M_0 = -10$ meV. The left and right leads are two normal quantum wires [29]. To calculate the conductance of such a junction, we first rewrite the tight-binding Hamiltonian of the junction in the square lattice. Then we calculate the conductance and current distribution by means of the lattice Green's function technique [29].

Figure 3 presents the numerical results of conductance and current distribution of an inverted T-shaped junction sketched in Fig. 2(a). The length of the 2DTI wire is $W_2 = 4000a$ (along the y direction) and the width is $L_1 = 31a$ (along the x direction, i.e., the transport direction), where a is the lattice constant. The width of the two leads is $W_1 = 30a$. The dispersion of edge states is shown in Fig. 3(a) where spin-up and spin-down edge states are degenerate. The finite-size effect induces the coupling between two edge states located at two edges and opens a small gap which is located near 7.5 meV. When incident electrons with the Fermi energy far below the gap (e.g., $E_F = 1$ meV) enter into the 2DTI from the left lead, only spin-down electrons can occupy the edge state to propagate upward along the edge. Without the electric field, spin-down electrons will be reflected to spin-up electrons by the top ferromagnet and then propagate downward, and finally go back to the left lead. In such a case, the conductance is zero. By applying a negative electric field, the potential can be decreased linearly along the 2DTI wire. If the electric field is big enough or the wire is long enough, there exists a region in the wire where the Fermi energy is located inside the gap. If the length of the region w is big enough, spin-down electrons will completely tunnel to the right edge according to Eq. (6). Now the conductance is a conductance quantum.

For a fixed finite-size-effect induced gap Δ, a big w means a weak electric field E_y due to $w = 2\Delta/E_y$. For a 2DTI ribbon with finite length W_2, the minimal potential difference between the bottom and the top should be $E_F - E_0$ to let the Fermi energy E_F cross the gap. Here E_0 denotes the energy of the center of gap. Therefore, the minimal electric field should be $(E_F - E_0)/W_2$. To make E_y small enough to get a quantized tunneling conductance, we need a big enough W_2. We consider a long 2DTI wire ($W_2 = 4000a$) to get a big w. The well-quantized conductances are obtained as functions of E_y for various E_F, as shown in Fig. 3(b). The electric field E_y causes a potential

drop along the wire from bottom to top. For small E_y, the conductance is 0 because the tunneling does not occur. When E_y is big enough that the potential drop is larger than the difference between the gap position and E_F (7.5 meV–E_F), there exists a region in the wire where E_F is located inside the gap. Now the conductance becomes 1 due to the tunneling between edge states. The tunneling is verified by the current distribution sketched in Fig. 3(c). The main tunneling position is exactly within the region where E_F lies inside the gap. Figure 3(d) shows that the quantized conductance is also robust against nonmagnetic disorders which are modeled by the random on-site potential uniformly distributed in the interval $[-U_{\mathrm{dis}}/2, U_{\mathrm{dis}}/2]$ [29].

Topological transistor based on interface state tunneling.—We also propose a topological transistor based on interface state tunneling as shown in Fig. 2(b). A normal insulator (NI) quantum wire with the size $L_2 \times W$ are sandwiched between two 2DTI leads with the same width W. The incident electrons from the edge states of left 2DTI either go back to the left lead or tunnel to the right lead through the interface state tunneling between two interfaces. The well-quantized conductance is shown in Fig. 4. The parameters for 2DTI leads for the same with those in Fig. 3. The NI is also described by Eq. (7) but with only one different parameter $M_0 = 10$ meV. The turn-on electric field exactly corresponds to the potential increase from bottom to top which equals to the difference between E_F and the gap [nearly $E_F - 0.5$ meV; see Figs. 4(a) and 4(b)]. The current distribution of spin-up electrons in Fig. 4(c) demonstrates the process of tunneling. The robustness of this tunneling effect is verified by the well-quantized conductance in the presence of nonmagnetic disorders, as shown in Fig. 4(d).

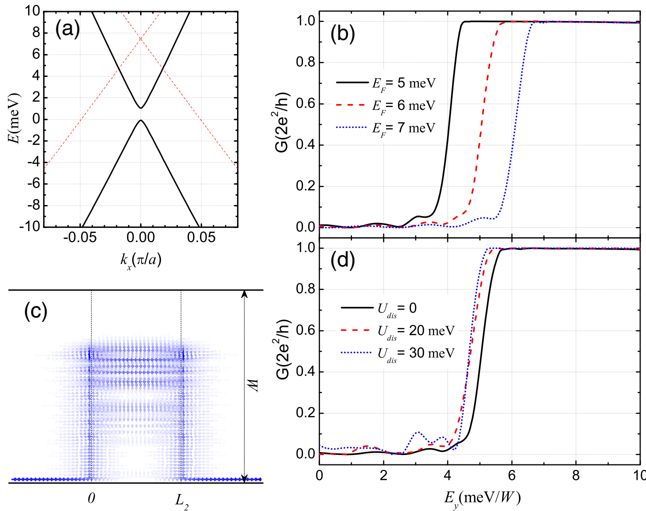

FIG. 4. Numerical results for the topological transistor based on interface state tunneling shown in Fig. 2(b). (a) Dispersion of a 2DTI/NI/2DTI quantum wire where a NI wire is sandwiched by two 2DTI wires. Solid black (dashed red) curves represent interface (edge) states. The width of the NI wire is $L_2 = 22a$. (b) Conductance as a function of E_y for three chosen Fermi energies $E_F = 5$, 6, and 7 meV. (c) Current distribution for $E_F = 6$ meV and $E_y = 7$ meV. Only spin-up electrons are considered. (d) Conductance in the presence of nonmagnetic disorders with various disorder strength U_{dis} for $E_F = 6$ meV. Structure parameters are $W = 4000a$ and $L_2 = 22a$.

Quantization conditions.—We give a brief guide to obtain well-quantized conductance in such topological transistors. For the off state, even E_F is far away from the gap, and there still exists a low probability that the tunneling will occur. The low probability is found to be Δ^2/E_F^2 [29]. To obtain a sufficiently small conductance in the off state, we first choose a suitable width L_1 or L_2 of the central device wire which should be small enough to induce a sufficiently small Δ, according to $\Delta = \Delta_0 e^{-2L/\xi}$. Then we determine the length of the device wire W_2 or W, which should be large enough to satisfy the condition $\Delta w/(\hbar v_F) \gg 1$ according to Eq. (6), which ensures a well-quantized conductance of 1 or 2 in the on state.

Experimental feasibility.—Finally, we comment on the experimental feasibility of proposed topological transistors. To achieve a quantized tunneling, the edge or interface channel should be ballistic before the tunneling. For 2DTIs, it has been experimentally found that the backscattering nearly always induces a deviation from the quantized conductance for a long edge channel [25,27,30,31]. The possible underlying mechanisms have been extensively discussed, including the presence of an external magnetic field or magnetic impurities, an $e-e$ interaction through the third order perturbation [32–34], the coupling of edge modes to charge puddles [35,36], the edge reconstruction [37], and the effects of Rashba spin-orbit coupling [38,39], phonons [40], nuclear spins [41,42], disordered probes [43], coupling to external baths [44], noise [45], etc. A significant breakthrough was made very recently [46]. It was shown that the combined action of short-range nonmagnetic impurities located near the edges and on-site electron-electron interactions effectively creates noncollinear magnetic scatterers and, hence, results in strong backscattering, even at zero temperature. Experimentally, both the spatially resolved study of backscattering using scanning gate microscopy [47] and the Hall bar measurement [48] reported the ballistic transport and quantized conductance in samples with an edge channel length up to 2 μm. The edge length dependence of the resistance indicates that the coherence length is up to 4.4 μm [48].

The numerical calculations show that the edge channels with length $4000a$ will promise a quantized tunneling. For InAs/GaSb quantum wells, the lattice constance is approximately 0.6 nm. The length of ballistic channels $4000a = 2.4$ μm is quite promising in experiments, though still a little more than the 2 μm reported so far. Moveover, because of the small band gap in HgTe/CdHgTe and InAs/GaSb quantum wells, the experimental observation of well-quantized tunneling conductance should be performed at

low temperature. The numerical calculations show that quantized tunneling conductance can persist at temperatures up to 10 K [29].

For a single edge, although the backscattering seems inevitable in a quite long quantum spin Hall edge channel, it is absent in a chiral edge channel because of the quantum anomalous Hall (QAH) effect. The reported ballistic channels in experiments are up to 2.4 mm in length [49]. Our proposed transistors can also work based on the tunneling between quantum anomalous Hall edge or interface states. For the transistor based on the QAH interface state tunneling, the setup is the same as that shown in Fig. 2(b). The results shown in Fig. 4 can also apply to QAH interface state tunneling, except with a change of the quantized conductance from 2 to 1. For the transistor based on the QAH edge state tunneling, we can propose a new longitudinal transistor which also possesses quantized conductances [29]. Therefore, the quantized tunneling effect should be also observable in transistors based on QAH insulators. It is worth noting that the search for QAH insulators at higher temperature, which in practice is smaller than the Curie temperature of ferromagnetism [50,51], is fast progressing [52,53].

More importantly, we note that a newly published work [54] reported the latest progress in the dissipationless transport of quantum spin Hall edge channels. Lunczer *et al.* successfully achieved quantized conductance even in long channels up to 13 μm in HgTe quantum well structures, through the flattening of the potential landscape by controlled gate training. With this technique, the use of quantized helical edge channel transport becomes feasible in macroscopic devices.

Conclusions.—In conclusion, we study in this Letter the tunneling between topological edge or interface states. It is found that the tunneling probability can be quantized and tunable by an electric field. We propose topological transistors based on edge or interface state tunneling in junctions including 2DTIs. The conductance can be quantized for a suitable size of the tunneling region and is also robust against nonmagnetic disorders. The proposed topological transistors are accessible in experiments and without topological transition in the operation. The finding sheds new light on the design of topological transistors.

The work described in this Letter is supported by the National Natural Science Foundation of China [(NSFC), Grants No. 11774144, No. 11774006, and No. 11574045], and the National Basic Research Program (NBRP) of China (Grant No. 2012CB921300).

*phjfliu@gzhu.edu.cn
†mazs@pku.edu.cn

[1] B. Zhou, H.-Z. Lu, R.-L. Chu, S.-Q. Shen, and Q. Niu, Phys. Rev. Lett. **101**, 246807 (2008).
[2] C. M. Wang, H.-P. Sun, H.-Z. Lu, and X. C. Xie, Phys. Rev. Lett. **119**, 136806 (2017).
[3] C. Zhang *et al.*, Nat. Commun. **8**, 1272 (2017).
[4] T. Schumann, L. Galletti, D. A. Kealhofer, H. Kim, M. Goyal, and S. Stemmer, Phys. Rev. Lett. **120**, 016801 (2018).
[5] C. Zhang *et al.*, Nature (London) **565**, 331 (2019).
[6] L. Andrew Wray, Nat. Phys. **8**, 705 (2012).
[7] M. Ezawa, Appl. Phys. Lett. **102**, 172103 (2013).
[8] J. Liu, T. H. Hsieh, P. Wei, W. Duan, J. Moodera, and L. Fu, Nat. Mater. **13**, 178 (2014).
[9] X. Qian, J. Liu, L. Fu, and J. Li, Science **346**, 1344 (2014).
[10] H. Pan, M. Wu, Y. Liu, and S. A. Yang, Sci. Rep. **5**, 14639 (2015).
[11] Q. Liu, X. Zhang, L. B. Abdalla, A. Fazzio, and A. Zunger, Nano Lett. **15**, 1222 (2015).
[12] Z. Zhang *et al.*, Nat. Nanotechnol. **12**, 953 (2017).
[13] A. Molle, J. Goldberger, M. Houssa, Y. Xu, S.-C. Zhang, and D. Akinwande, Nat. Mater. **16**, 163 (2017).
[14] A. M. Kadykov *et al.*, Appl. Phys. Lett. **107**, 152101 (2015).
[15] M. Ezawa, Phys. Rev. Lett. **121**, 116801 (2018).
[16] S. Guan, Z.-M. Yu, Y. Liu, G.-B. Liu, L. Dong, Y. Lu, Y. Yao, and S. A. Yang, npj Quantum Mater. **2**, 23 (2017).
[17] S. S. Krishtopenko, I. Yahniuk, D. B. But, V. I. Gavrilenko, W. Knap, and F. Teppe, Phys. Rev. B **94**, 245402 (2016).
[18] A. M. Kadykov, S. S. Krishtopenko, B. Jouault, W. Desrat, W. Knap, S. Ruffenach, C. Consejo, J. Torres, S. V. Morozov, N. N. Mikhailov, S. A. Dvoretskii, and F. Teppe, Phys. Rev. Lett. **120**, 086401 (2018).
[19] Z. Wang, J. Song, H. Liu, H. Jiang, and X. C. Xie, New J. Phys. **17**, 113040 (2015).
[20] Y. Xu, S. Uddin, J. Wang, J. Wu, and J.-F. Liu, Sci. Rep. **7**, 7578 (2017).
[21] V. Krueckl and K. Richter, Phys. Rev. Lett. **107**, 086803 (2011).
[22] J. Maciejko, E.-A. Kim, and X.-L. Qi, Phys. Rev. B **82**, 195409 (2010).
[23] F. Dolcini, Phys. Rev. B **83**, 165304 (2011).
[24] W. G. Vandenberghe and M. V. Fischetti, Nat. Commun. **8**, 14184 (2017).
[25] M. König, S. Wiedmann, C. Brüne, A. Roth, H. Buhmann, L. W. Molenkamp, X.-L. Qi, and S.-C. Zhang, Science **318**, 766 (2007).
[26] M. König, H. Buhmann, L. W. Molenkamp, T. L. Hughes, C.-X. Liu, X.-L. Qi, and S.-C. Zhang, J. Phys. Soc. Jpn. **77**, 031007 (2008).
[27] A. Roth, C. Brüne, H. Buhmann, L. W. Molenkamp, J. Maciejko, X.-L. Qi, and S.-C. Zhang, Science **325**, 294 (2009).
[28] M. Ezawa and N. Nagaosa, Phys. Rev. B **88**, 121401(R) (2013).
[29] See Supplemental Material at http://link.aps.org/supplemental/10.1103/PhysRevLett.123.206801 for the lattice Hamiltonians of two proposed topological transistors, the numerical methods to calculate the conductance and current distribution, the estimation of the tunneling probability in the off state, the transistor based on quantum anomalous Hall edge states, and the temperature dependence of tunneling conductance.

[30] K. Suzuki, Y. Harada, K. Onomitsu, and K. Muraki, Phys. Rev. B **87**, 235311 (2013).
[31] G. Grabecki *et al.*, Phys. Rev. B **88**, 165309 (2013).
[32] C. Xu and J. E. Moore, Phys. Rev. B **73**, 045322 (2006).
[33] C. Wu, B. A. Bernevig, and S.-C. Zhang, Phys. Rev. Lett. **96**, 106401 (2006).
[34] T. L. Schmidt, S. Rachel, F. von Oppen, and L. I. Glazman, Phys. Rev. Lett. **108**, 156402 (2012).
[35] J. I. Väyrynen, M. Goldstein, and L. I. Glazman, Phys. Rev. Lett. **110**, 216402 (2013).
[36] J. I. Väyrynen, M. Goldstein, Y. Gefen, and L. I. Glazman, Phys. Rev. B **90**, 115309 (2014).
[37] J. Wang, Y. Meir, and Y. Gefen, Phys. Rev. Lett. **118**, 046801 (2017).
[38] A. Ström, H. Johannesson, and G. I. Japaridze, Phys. Rev. Lett. **104**, 256804 (2010).
[39] F. Crépin, J. C. Budich, F. Dolcini, P. Recher, and B. Trauzettel, Phys. Rev. B **86**, 121106(R) (2012).
[40] J. C. Budich, F. Dolcini, P. Recher, and B. Trauzettel, Phys. Rev. Lett. **108**, 086602 (2012).
[41] C.-H. Hsu, P. Stano, J. Klinovaja, and D. Loss, Phys. Rev. B **96**, 081405(R) (2017).
[42] C.-H. Hsu, P. Stano, J. Klinovaja, and D. Loss, Phys. Rev. B **97**, 125432 (2018).
[43] A. Mani and C. Benjamin, Phys. Rev. Applied **6**, 014003 (2016).
[44] A. A. Bagrov, F. Guinea, and M. I. Katsnelson, arXiv:1805.11700.
[45] J. I. Väyrynen, D. I. Pikulin, and J. Alicea, Phys. Rev. Lett. **121**, 106601 (2018).
[46] P. Novelli, F. Taddei, A. K. Geim, and M. Polini, Phys. Rev. Lett. **122**, 016601 (2019).
[47] M. König *et al.*, Phys. Rev. X **3**, 021003 (2013).
[48] L. Du, I. Knez, G. Sullivan, and R.-R. Du, Phys. Rev. Lett. **114**, 096802 (2015).
[49] C.-Z. Chang, W. Zhao, D. Y. Kim, P. Wei, J. K. Jain, C. Liu, M. H. W. Chan, and J. S. Moodera, Phys. Rev. Lett. **115**, 057206 (2015).
[50] X. Zhang and S.-C. Zhang, Proc. SPIE Int. Soc. Opt. Eng. **8373**, 837309 (2012).
[51] B. Shabbir, M. Nadeem, Z. Dai, M. S. Fuhrer, Q.-K. Xue, X. Wang, and Q. Bao, Appl. Phys. Rev. **5**, 041105 (2018).
[52] Y. Deng, Y. Yu, M. Z. Shi, J. Wang, X. H. Chen, and Y. Zhang, arXiv:1904.11468.
[53] C. Tang, C.-Z. Chang, G. Zhao, Y. Liu, Z. Jiang, C.-X. Liu, M. R. McCartney, D. J. Smith, T. Chen, J. S. Moodera, and J. Shi, Sci. Adv. **3**, e1700307 (2017).
[54] L. Lunczer, P. Leubner, M. Endres, V. L. Müller, C. Brüne, H. Buhmann, and L. W. Molenkamp, Phys. Rev. Lett. **123**, 047701 (2019).